

FORMATION AND MECHANICS OF  
SELF-ASSEMBLED MOLECULAR GELS

BY

NIKOLA DUDUKOVIC

THESIS

Submitted in partial fulfillment of the requirements  
for the degree of Master of Science in Chemical Engineering  
in the Graduate College of the  
University of Illinois at Urbana-Champaign, 2013

Urbana, Illinois

Advisor:

Professor Charles F. Zukoski

## ABSTRACT

Molecular gels are associated with the formation of space spanning structures produced by aggregation of low molecular weight molecules that associate through hydrogen bonding,  $\pi$ -stacking, acid base or van der Waals interactions. One specific type of gel forming molecule is based on a hydrophobic peptide – fluorenylmethoxycarbonyl diphenylalanine (Fmoc-FF). This thesis explores gels formed when water is added to Fmoc-FF dissolved in dimethyl sulfoxide (DMSO). At high water concentrations, gels are formed at concentrations as low as 0.001%. We establish the gel line defining the Fmoc-FF and water concentrations where gels are formed. At fixed water concentration, over a narrow range of Fmoc-FF concentrations, solutions pass from being low viscosity liquids to a rigid material with elastic moduli  $G' > 10^5$  Pa. Here we characterize the kinetics of gelation and demonstrate that these gels are reversible in the sense that they can be disrupted mechanically and will rebuild strength over time. We attempt to understand the gelation process as arising from increasing strength of attraction between Fmoc-FF molecules with increasing water concentration. Furthermore, an effort is made to describe the underlying changes in strength of attraction leading to gelation and the mechanical behavior of the resulting gels using a dynamic localization theory.

# TABLE OF CONTENTS

List of Symbols .....	v
Chapter 1. Introduction .....	1
1.1. Gels – Basic Definitions .....	1
1.2. Molecular Gels – Structure and Properties .....	3
1.3. Motivation and Goals .....	4
Chapter 2. Colloidal Gel Theories .....	6
2.1. Mode Coupling Theory .....	6
2.2. Localization Models .....	7
2.2.1. Schweizer Ultralocal Limit Model .....	7
2.2.2. Bergenholtz-Fuchs Model for Dilute Systems .....	9
2.2.3. Summary of Localization Theories .....	10
Chapter 3. Materials and Experimental Methods .....	12
3.1. Fmoc-diphenylalanine .....	12
3.2. Gel Preparation .....	13
3.3. Controlling Strength of Attraction with Water Concentration .....	13
3.4. Titration Experiments .....	14
3.5. Rheological Measurements .....	14
Chapter 4. Results and Discussion .....	16
4.1. State Behavior .....	16
4.2. Elastic and Viscous Moduli Measurements .....	18
4.2.1. Gel Formation .....	18
4.2.2. Dependence on Fmoc-FF and Water Concentration .....	19
4.2.3. Gel Reversibility .....	22

4.3. Comparison with Ultralocal Limit Model .....	23
4.3.1. Relating Strength of Attraction with Water Concentration and Gel Point Prediction .....	24
4.3.2. Scaling Arguments and Elastic Modulus Prediction .....	26
Chapter 5. Conclusions .....	30
5.1. Experimental and Modeling Observations .....	30
5.2. Future Studies .....	31
References .....	33

# LIST OF SYMBOLS

$C(k)$	Fourier transformed direct correlation function
$g$	Pair distribution function
$G'$	Elastic modulus
$G''$	Viscous modulus
$k$	Boltzmann constant
$m$	Mass
$r_L$	Localization length
$S(k)$	Collective structure factor
$T$	Temperature
$V$	Volume
$x(\text{H}_2\text{O})$	Water concentration (volume fraction)
$\varepsilon$	Strength of attraction
$v_\infty$	Coupling constant
$\sigma$	Particle size
$\phi$	Particle volume fraction

# CHAPTER 1. INTRODUCTION

## 1.1. Gels – Basic Definitions

Gels are multi-component materials with long mechanical relaxation times that can be deformed with modest stresses. These materials hold their shape, but possess yield stresses, which allows them to be squeezed out of tubes, easily applied to sensitive tissues and pumped long distances at low viscosity. Due to their soft nature, gels have applications in personal care products (toothpaste, shampoo, deodorants, etc.), food industry (syrups, puddings, jelly, etc.), electronic devices, drug delivery, tissue engineering, mineral processing, waste handling and oil production [1]. Gelation is the conversion of a liquid to a disordered solid by formation of a network of chemical or physical bonds between the molecules or particles composing the liquid [2]. For a system to gel, connectivity may be introduced such that it is practically irreversible (e.g., chemical bond) or reversible (e.g., physical junction, long range self-organization). In disruption of gels, the disconnecting process may also be irreversible (e.g., mechanical breaking of chemical bonds, thermal degradation) or reversible (e.g., thermally induced phase transitions, mechanical degradation for structures which can reform). Different time scales and driving mechanisms govern the phenomena of gelation and disruption of gels so that they cannot be considered to be mutually symmetric [3].

In polymer gels, the gel transition is associated with chemical gelation, in which crosslinking of a polymer (the formation of irreversible chemical bonds between different polymer chains) results in the formation of a space-spanning network with finite shear modulus and infinite viscosity. The chemical gelation process has been described by percolation theory, in which the gel point is defined by the appearance of an infinite spanning network. Percolation theory is based on the probability of independent bond formation under the assumption of the absence of bonding loops. At the time of reaction

when the system reaches the gel point, a fraction  $\alpha_{\text{gel}}$  of possible bonds is formed, and at this point the system percolates. Chemically gelling systems exhibit slow relaxation approaching the gel transition that can be fitted by an exponential decay, and a power law decay of the density correlation function close to percolation.

Physical gelation occurs as a result of intermolecular association, leading to network formation. These gels are usually formed by colloidal particles, as well as associative polymers. Typically, a colloidal gel is coherent mass consisting of a liquid in which particles are either dispersed or arranged in a network throughout the mass. A gel may be notably elastic and jellylike (such as gelatin or fruit jelly) or quite solid and rigid (such as silica gel). Bonds in these systems can be induced by thermal effects, depletion interactions, hydrogen bonds, hydrophobic effects, etc. and have shorter lifetimes compared to chemical bonds, i.e. the bonds are transient and particle clusters can form, break and reform in substantially shorter time periods that is consistent with the formation of covalent bonds. Colloidal gel formation is often based on weak attractive potentials. When strength of attraction is increased (for example, by lowering temperature), the system tends to shift into a state of minimal energy, which results in localized configurations.

In physical gelation of colloidal systems, the dynamical arrest can differ depending on the presence or absence of the colloid-rich and colloid-poor phase separation. Like a single component molecular system, as the thermal energy becomes comparable to the strength of intermolecular attraction, colloidal suspensions can undergo liquid-liquid or liquid-solid phase transitions. Gelation arises under the same conditions and can often occur at modest volume fraction near or within the spinodal of an equilibrium liquid-liquid phase separation. Distinguishing between the origin of gelation as occurring as the result of a quenched spinodal phase separation or occurring due to dynamical arrest can be difficult. These routes to colloidal gelation are often referred to as ‘non-equilibrium’ and ‘equilibrium’ routes, respectively. Non-equilibrium gels are expected to continuously evolve towards their lowest free energy of dense and dilute colloidal phases. Equilibrium gelation is not driven by the existence of a lower free energy state; gelation is a dynamical property of the system. As a result, from a global

free energy perspective, densification of localized structures is not more favored than particle dispersion.

## 1.2. Molecular Gels – Structure and Properties

Low molecular weight gelators confer enhanced viscosities and long stress relaxation times at very low volume fractions. The gelation process is associated with the formation of space spanning structures formed by aggregation of the gelator molecules through hydrogen bonding and  $\pi$ -stacking interactions. These short-range interactions, physical and thermoreversible in nature, result in strongly anisotropic structures of fibrils and ribbons that branch to fill space form the gel structure.

When low molecular weight gelators are added at some concentration and the gelation process is triggered (usually by a change in pH or temperature), the gelator molecules self-assemble through aggregation involving highly specific interactions that allow preferential pseudo-one-dimensional growth, usually favoring fibers (but allowing branching) that serve the function of the polymer chains in polymer gels. The “junction zones” between fibers, whose shapes may be in the form of strands, tapes, chiral ribbons, tubules or other aggregates with very large aspect ratios, provide rigidity to the microstructure. The resulting network forms a three-dimensional porous lattice that permeates the volume of the sample, encapsulating the liquid component and inhibiting its flow. The interactions responsible for holding the network together are non-covalent in nature [4].

These low molecular gelators can be inorganic or organic. In many cases, gelation arising from the presence of inorganic gelators features formation of new covalent bonds in the aggregation process, resulting in irreversible gels. Organic gelators confer non-covalent interactions that enable reversible gelation, i.e. the gels can be mechanically or thermally disrupted back into liquid and reform to their original state.



One particularly interesting group of molecular gels are ones arising from the self-assembly of peptide based molecular gelators. In peptide based nanomaterials, the structure formed by a single peptide can interact with another complementary peptide via non-covalent interactions: ionic, hydrophobic, hydrogen bonding and  $\pi$ -stacking. When a large number of these building blocks are contained, supramolecular structures can be formed. Ulijn *et al.* have found that short dipeptide derivatives with an added aromatic group, such as a carbobenzyloxy, naphthalene, or fluorenylmethoxycarbonyl group, can self-assemble into stable hydrogels that possess characteristic solid-like gel rheological behavior [5-8]. Similar results have been found in several other studies [9-17].

The origin of these molecular gels is not well understood and there are several possibilities of why the gel formation occurs. Under the hypothesis that gels based on organic molecular gelators have similar characteristics and behavior as colloidal gel, one possible reason is that gelation could arise from crystallization, which occurs when the strength of short range attractions between particles is increased. However, if the crystalline state is not the equilibrium, minimum free energy structure, the system will undergo liquid-liquid phase separation. Gelation could arise from arrested phase separation if the system is quenched into the spinodal, resulting in a metastable gel. The gel could also be a result of disrupted phase separation due to patchy interactions between particles with valency limitations. These systems are characterized by the absence of the spinodal and increasing the strength of attraction should lead to an equilibrium state where particles are localized in clusters or form structures that fill space.

### 1.3. Motivation and Goals

In the last decade, molecular gels have seen an increasing number of potential application – in tissue engineering, drug delivery, nanofabrication, biological applications,

etc. [5, 8, 11, 14, 18]. The main advantage of molecular gelators and the reason for their versatility is that they can be synthesized to feature unique structural, optical, and biological functionality. Additionally, they allow formation of stiff gels at very low volume fractions ( $< 1\%$ ). This means that for many applications where modification of flow properties can be achieved with addition of tiny amounts of material.

However, despite this ability to synthesize low molecular gelators, the principles of their assembly remain poorly understood thus limiting control of gel stability and the generalization of the principles of gel formation that would lead to broader functional materials. One of the main criteria for potential application of molecular gels is their stability. The lifetime of the gel at room temperature, as well as thermal stability, resistance to mechanical disruption and reversibility are all of great importance for the overall usefulness of the gel. The stability of the gel depends on the nature of the interactions between its constituents. If the gel is formed from a metastable structure, it will destabilize over time and revert to its equilibrium state. Thus, it is of considerable importance to be able to understand and control the thermodynamic state of molecular gels.

To the best of our knowledge, there has not yet been a study of gelation and mechanical properties of molecular gels, carried out in a systematic way with the goal of understanding the underlying principles of gel formation and behavior. Therefore, the main objectives of this work were:

1. Controlling the strength of attraction and molecular gelator volume fraction in order to determine critical gelator concentration at which the gel point is reached.
2. Investigating the effect of gelator volume fraction and strength of attraction on the mechanical properties of the gel by means of rheological measurements.
3. Probing the reversibility of dipeptide based molecular gels upon mechanical disruption.
4. Developing a theoretical model capable to predict the gel point and mechanical behavior of the molecular gel.

## CHAPTER 2. COLLOIDAL GEL THEORIES

### 2.1. Mode Coupling Theory

Mode Coupling Theory (MCT) was developed in the 1970s by Bengtzelius, Götze and Sjölander as an effort to find a correct quantitative description of the dynamics of dense simple liquids. By using mode-coupling approximations, equations of motion for density correlation functions can be derived and their solutions give at least a semi-quantitative description of the dynamics of the system. One of the particularly significant features of MCT equations is that they give a qualitative description of the so-called “cage effect” – the phenomenon where in a dense liquid a particle is temporarily trapped by its neighbors and that it takes the particle some time to escape this cage. The main advantage of MCT over other glass transition theories is the fact that it makes a number of predictions that can be tested in experiments or computer simulations, in contrast to most other theories which make far fewer predictions and for which it is therefore much harder to be put on a solid experimental foundation [19].

MCT features a closed set of coupled equations for the intermediate scattering function, which describes the length scale dependent decay of correlations in density fluctuations, the mode-coupling equations, whose solution gives a time dependence of the intermediate scattering function. It is believed that they give a correct description of the dynamics of a particle at short times, i.e. when it is still in the cage that is formed by its neighbors at time zero, and of the breaking up of this cage at long times, i.e. up to the time scales when the particle finally shows a diffusive behavior.

## 2.2. Localization Models

### 2.2.1. Schweizer Ultralocal Limit Model

Schweizer *et al.* have developed a dynamic localization theory for describing the glass transition of colloidal particles [20-30]. A model was designed suggesting a limiting version of the barrier hopping theory that focuses only on the short range aspect of the dynamics, i.e. hard core collisions (referred to as the “ultralocal limit”) [31]. The model is able to predict the localization length ( $r_L$ ) as a function of particle size ( $\sigma$ ), particle volume fraction ( $\phi$ ) and strength of attraction ( $\epsilon$ ). The subsequent predictions that can be made include the gel point  $\phi_{gel}$  and the elastic modulus  $G'$ .

The theory reduces to naive MCT for the long time limit of the particle displacement or localization length  $r_L$ :

$$r_L^{-2} = \frac{1}{9} \int \frac{dk}{(2\pi)^3} \rho k^2 C^2(k) S(k) \exp\{-k^2 r_L^2 (1 + S^{-1}(k)) / 6\} \quad (1)$$

After a series of mathematical operations, the localization equation can be written as:

$$\left(\frac{\sigma}{r_L}\right)^2 = \frac{\sqrt{3\pi}}{72\pi^2} v_\infty \frac{\sigma}{r_L} \operatorname{erfc}(k_c r_L / \sqrt{3}) \quad (2)$$

where  $v_\infty$  is a coupling constant proportional to the mean square effective force exerted on a tagged particle. For hard spheres:

$$v_{\infty} = 96\pi\phi g^2(\sigma) \quad (3)$$

where  $g(\sigma)$  is the contact value of the pair distribution function. Here an approximation is made that for particles experiencing short range attractions with a strength of  $\varepsilon$ . The contact value of the pair distribution function can be written:

$$g(\sigma) = g^{HS}(\sigma)e^{\varepsilon/kT} \quad (4)$$

where  $g^{HS}(\sigma)$  is the hard sphere pair distribution function at contact, which is a function of particle volume fraction:

$$g^{HS}(\sigma) = \frac{1 + \phi/2}{(1 - \phi)^2} \quad (5)$$

With these approximations, the elastic modulus can be written:

$$G' = \rho kT \frac{\sqrt{3\pi}}{240\pi^2} v_{\infty} \frac{\sigma}{r_L} = \frac{9}{5\pi} \frac{\phi kT}{\sigma r_L^2} \quad (6)$$

Thus, when a particle size is specified, if one knows the attraction energy, the gel point can be found, corresponding to the first finite value of  $r_L$ . In the low volume

fraction limit of particular interest here, the model predicts a scaling of  $1/r_L \sim \phi^2$  such that  $G' \sim \phi^3$ .

### 2.2.2. Bergenholtz-Fuchs Model for Dilute Systems

Bergenholtz and Fuchs have developed a model describing asymptotic behavior of particles interacting via a hard core plus an attractive Yukawa tail, sometimes referred to as the hard-core attractive Yukawa (HCAY) system, used with mean spherical approximation (MSA) [32]. For HCAY systems, the interaction potential is given by:

$$u(r) = \begin{cases} \infty & r < \sigma \\ -K \frac{k_B T}{r/\sigma} \exp[-b(r/\sigma - 1)] & r > \sigma \end{cases} \quad (7)$$

where the dimensionless parameters  $K$  and  $b$  determine the strength and range of the attraction, respectively. For dilute systems, the model predicts a scaling of  $G' \sim \phi^2$ :

$$G' \approx 0.0764 b \phi^2 K^2 k_B T / \sigma^3 \quad (8)$$

The differences between the Bergenholtz and Fuchs result and the ultralocal limit result from different approximations made for  $S(q)$  and descriptions of the direct correlation function. The point is that the asymptotic behavior at low volume fraction is very sensitive to the pair potential and approximations made in approaching the low volume fraction limit.

### 2.2.3. Summary of Localization Theories

- The localization theories are based on equilibrium descriptions of solution structure. They do not recognize the existence of other equilibrium phases and thus characterize localization outside a spinodal. They also are limited to rapid quenches if gelation occurs in a metastable state between a liquid and crystalline phase.
- The models have been developed for spherical particles experiencing centrosymmetric pair potentials and can predict localization at very low volume fractions.
- The dependence of the elastic modulus on the volume fraction of particles is very sensitive to the details of the pair potential experienced by the particles as well as the approximations used to solve the mode coupling equations.
- Both models predict that at a specific volume fraction and strength of attraction the system will experience a localization event. In the Schweizer model this occurs with the formation of a dynamic potentials and the crossover volume fraction is not observable dynamically. However, as volume fraction is raised, the dynamic potential develops a minimum at  $r_L$ , which grows in magnitude with volume fraction and rapidly slows relaxation processes. For large strengths of attraction that give rise to low volume fractions at gelation, these changes occur over a very narrow volume fraction range.
- These models suggest that  $\phi_{gel}$  is a function of strength of attraction and particle size and that from this volume fraction one can predict  $G'_{gel}$  to within a constant associated with the size of the particles in the system.

- Each model predicts that in the limit of low volume fraction (or strong strengths of attraction) one expects gels to have common properties where  $G' \sim \phi^x$  where  $x$  is independent of volume fraction and strength of attraction. As a result, one expects  $G' \sim G'_{gel} \phi^x$ , where  $G'_{gel}$  contains all information about the strength and range of the attraction.

These models based on mode coupling are the only available theories that will predict both the localization volume fraction and the volume fraction dependence of the modulus above the gel point. The models have not been adapted to particles experiencing anisotropic interactions and certainly cannot be used to predict the properties of a nonequilibrium gel or a gel composed of equilibrium phase-separated but interwoven fibers. Thus, applying these models to Fmoc-FF is at best an attempt to rationalize a great deal of consistent data.



## CHAPTER 3. MATERIALS AND EXPERIMENTAL METHODS

### 3.1. Fmoc-diphenylalanine

The dipeptide based molecular gelator chosen for this study was N-fluorenylmethoxycarbonyl diphenylalanine (Figure 1), or Fmoc-FF from hereon, with a molecular weight of 534.61 g/mol. The aromatic Fmoc-group serves as a protective group for amines, while the two phenylalanine groups result in considerably high overall hydrophobicity of the molecule ( $\log P = 5.574$ ) [9]. The material was purchased from Bachem at 99% purity. At room temperature, it is a solid white substance and soluble in various organic solvents. In this study, dimethyl sulfoxide (DMSO) of purity 99.5% was used as a solvent. All experiments were performed with Milli-Q deionized water.

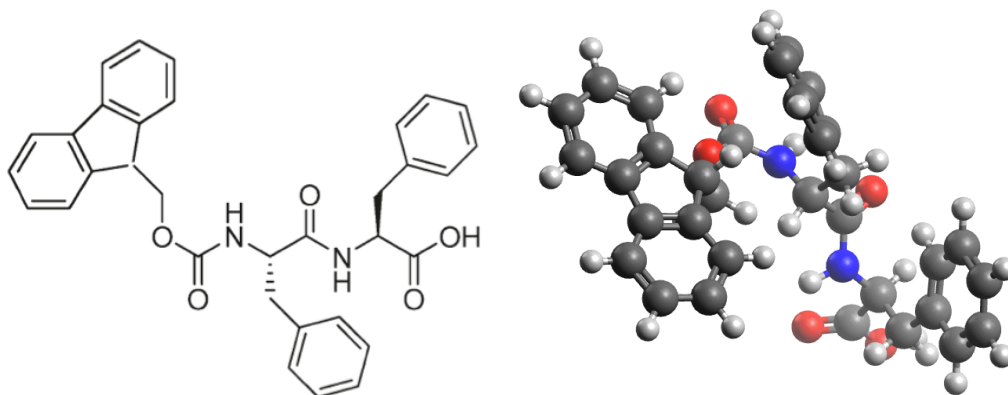


**Figure 1.** Molecular structure of Fmoc-FF.

## 3.2. Gel Preparation

The mass of required Fmoc-FF in solid form was measured on a scientific electronic scale with 0.0001 g precision. The measured amounts of Fmoc-FF were dissolved in DMSO at selected concentrations, after which the samples were vortex mixed for 2 minutes until a clear solution was obtained. The solutions were then mixed with water at various ratios in order to obtain the desired final concentrations. All gels used in the experiments were prepared at room temperature.

## 3.3. Controlling Strength of Attraction with Water Concentration

Since Fmoc-FF molecules self-assemble into networks at room temperature, it is necessary to control the strength of attraction between the molecules in a way that does not involve temperature quenching of any kind. The trigger fused here for the self-assembly process is the addition of water to the Fmoc-FF solution, and the underlying driving force is the high hydrophobicity of the Fmoc-FF molecules due to the presence of two hydrophobic phenylalanine groups. Previous studies suggest that the addition of water drives the hydrophobic particles closer together, allowing them to form  $\beta$ -sheets which spiral out into fibers that branch out, thus forming a space filling network.

From these studies, we arrive to the assumption is that particle-particle interactions can be systematically varied by altering the amount of water at a fixed Fmoc-FF concentration in the final gel. A higher water concentration is expected to cause a greater hydrophobic effect, driving the hydrophobic particles closer together where short range interactions take over.

### 3.4. Titration Experiments

In order to establish how the location of the gel transition, i.e. to determine the relationship between critical Fmoc-FF and water concentrations that give rise to gel formation, titration experiments were performed. Solutions of Fmoc-FF in DMSO of 1 mL volumes were prepared at selected concentrations in 7 mL vials. Each solution was then titrated with 10  $\mu$ L droplets of deionized water, followed by mixing and a waiting time of 1 minute, until a gel was formed. The adopted criterion for establishing gel formation was that the sample did not exhibit flow within a time of one minute after each water droplet addition. The experimental results and observations are presented in section 4.1.

### 3.5. Rheological Measurements

All rheology experiments were performed on a Bohlin rheometer equipped with a thermostat (set at 25 °C). The setup used for the experimental measurements was a cone and plate geometry (4°/40 mm cone). The gel samples were applied by first preparing the appropriate Fmoc-FF solution, followed by mixing it with water in the desired ratio, then pouring the still liquid sample onto the plate before the gel transition occurs and lowering the cone into measurement position.

The elastic (storage) modulus and viscous (loss) modulus were measured at a constant shear stress (100 Pa) and frequency (1 Hz). In order to examine the effect of gelator and water concentration on the mechanical properties of the gel, the measurements were performed using a systematic approach where:

1. The water concentration was kept fixed and experiments were performed on samples with a range of concentration around the gel point.
2. The Fmoc-FF concentration in the final gel was kept fixed and the water concentration was varied around the gel point.

Gel reversibility was investigated by inducing high shear stress on the sample in order to cause it to yield. A constant shear stress (50 Pa) was applied at constant frequency (1 Hz) until the gel was fully formed (indicated by a constant value of the elastic modulus). Then, shear stress of 550 Pa was applied at the same constant frequency until the gel yielded, which was indicated by the viscous modulus becoming greater than the elastic modulus. Once the sample had yielded, the shear stress was reverted to its original value of 50 Pa and the elastic and viscous moduli were monitored to observe whether the gel is reforming. The results of the rheological measurements are presented in section 4.2.

## CHAPTER 4. RESULTS AND DISCUSSION

### 4.1. State Behavior

The adopted criterion for establishing gel formation was that the sample did not exhibit flow within a time of one minute after each water droplet addition. As the gel point is approached, the mixing of water and clear Fmoc-FF/DMSO solution leads to a quick transition of the mixture into a turbid, opaque white solution. The observed opacity indicates the presence of structures of sizes large enough to scatter light. Below the gel point, the opaque solution occurring upon mixing changes to a clear liquid, implying an absence of the initial large structures. At the gel point, the system stops flowing and becomes solid-like. The gel transition can be visually observed by a gradual shift from an opaque white solution into a transparent gel (Figure 2). This suggests that the molecules forming the initial large particle clusters reorganize into a network of smaller dimensions (such as nanofibers), resulting in a transparent gel.



**Figure 2.** Fmoc-FF gel preparation and opaque-clear transition.

The results of the titration experiments described in section 3.4. are given in Figure 3. The data points, representing gel points, were obtained by moving along a diagonal line between pure water ( $x(\text{H}_2\text{O}) = 1$ ) and pure Fmoc-FF/DMSO solutions of various concentrations. Gels are formed along a line of increasing Fmoc-FF volume fraction and decreasing water concentration. The solubility curve exhibits a power law behavior and it can be seen that stable gels can be obtained even at extremely low volume fractions of Fmoc-FF (less than  $5 \times 10^{-4}$ ).

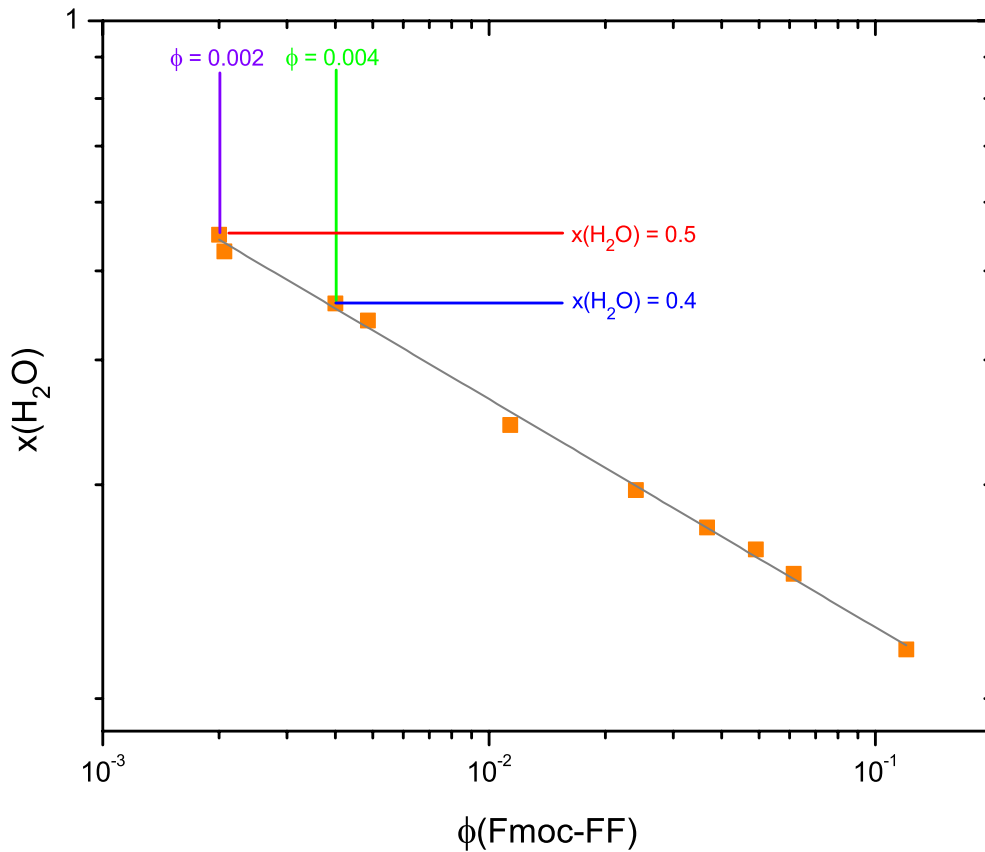


**Figure 3.** Gelation curve obtained by titration experiments. The data points represent gel points at different concentrations, i.e. the first point for which the samples exhibit no flow after a waiting time of 1 minute. The gelation curve exhibits an exponential behavior of the form:  $x(\text{H}_2\text{O})_{gel} = 0.0764 (\phi(\text{Fmoc-FF})_{gel})^{-0.286}$ .

The volume fraction of Fmoc-FF in the gel was calculated under the assumption of ideal mixing as:

$$\phi(\text{Fmoc-FF}) = \frac{(m/\rho)_{\text{Fmoc-FF}}}{V_{\text{H}_2\text{O}} + V_{\text{DMSO}} + (m/\rho)_{\text{Fmoc-FF}}} \quad (9)$$

where  $\rho_{\text{Fmoc-FF}} = 1273 \text{ g/L}$  is the density of Fmoc-diphenylalanine. For further experimental investigations, two gel points have been chosen:

- $\phi(\text{Fmoc-FF}) = 0.002$  and  $x(\text{H}_2\text{O}) = 0.5$
- $\phi(\text{Fmoc-FF}) = 0.004$  and  $x(\text{H}_2\text{O}) = 0.4$

The effects of gelator and water concentration will be examined around these two gel points, along lines of constant Fmoc-FF concentration in the final gel (at fixed water concentration) and lines of constant water concentration (at fixed Fmoc-FF).

## 4.2. Elastic and Viscous Moduli Measurements

### 4.2.1. Gel Formation

As previously described, rheological experiments in which the elastic and viscous moduli were measured were performed on samples of varying Fmoc-FF and water concentrations. The oscillation measurements at constant frequency (1 Hz) and constant shear stress (100 Pa) revealed that, even though the gel transition for all samples occurred in less than 5 minutes, the gels were not fully formed until a number of hours later. This can be observed in the growth of the elastic modulus with time (Figure 4). It can be seen that the elastic modulus quickly jumps to a very high value when the gel is initially formed, but only reaches a constant value after a few hours. This behavior indicates a

drastic slowing down of the diffusion kinetics, which could mean that during this time, the fibrous network is still branching, thereby increasing the gel stiffness, and is only fully formed once the value of the elastic modulus becomes constant.

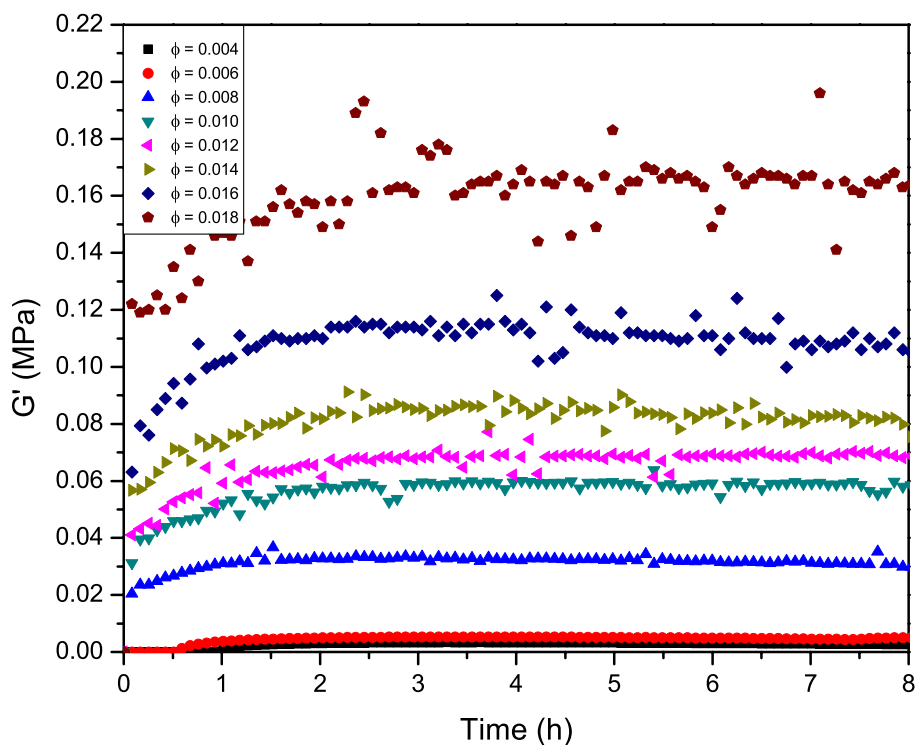


**Figure 4.** Stiffening of gels of different Fmoc-FF concentrations at  $x(\text{H}_2\text{O}) = 0.4$  with time.

#### 4.2.2. Dependence on Fmoc-FF and Water Concentration

As seen from Figure 4, the obtained elastic modulus values are on the order of magnitude of  $10^5$  Pa, which can be considered very high for such low gelator concentrations (typical colloidal gels usually have moduli on the order of a few thousand Pa in this concentration range). Furthermore, there is a clear trend of increasing gel



stiffness (elastic modulus) with increasing Fmoc-FF concentration. A similar trend can be observed for varying Fmoc-FF concentrations at  $x(\text{H}_2\text{O}) = 0.5$  (Figure 5). When rescaled by the modulus at gel point and the volume fraction of Fmoc-FF at the gel point, both of these data series fit to a single power law with a slope of  $\sim 2.5$  (Figure 6).

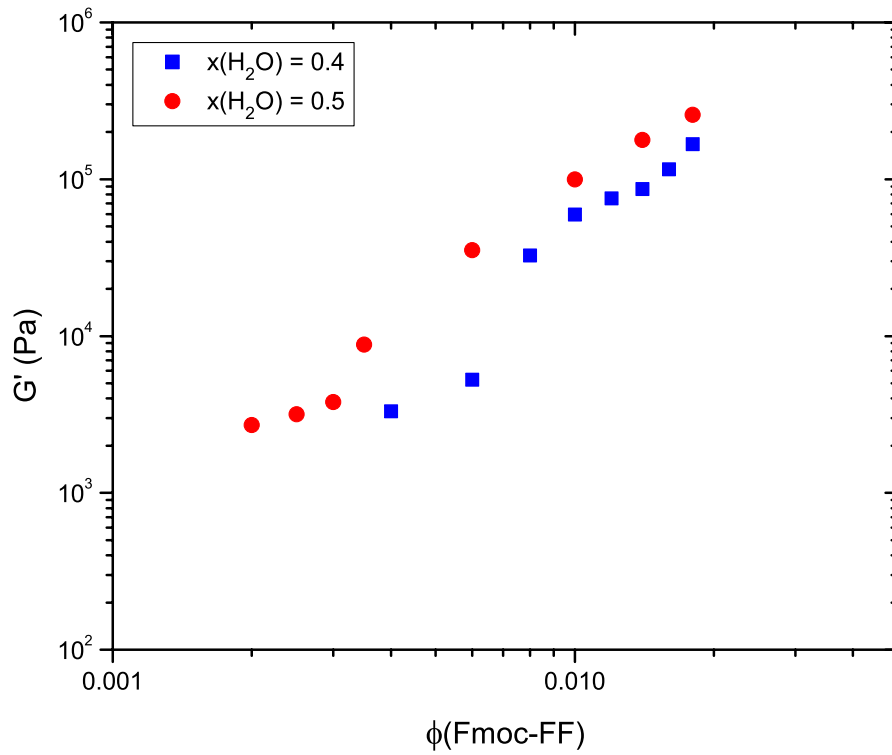


**Figure 5.** Dependence of elastic modulus on Fmoc-FF volume fraction.

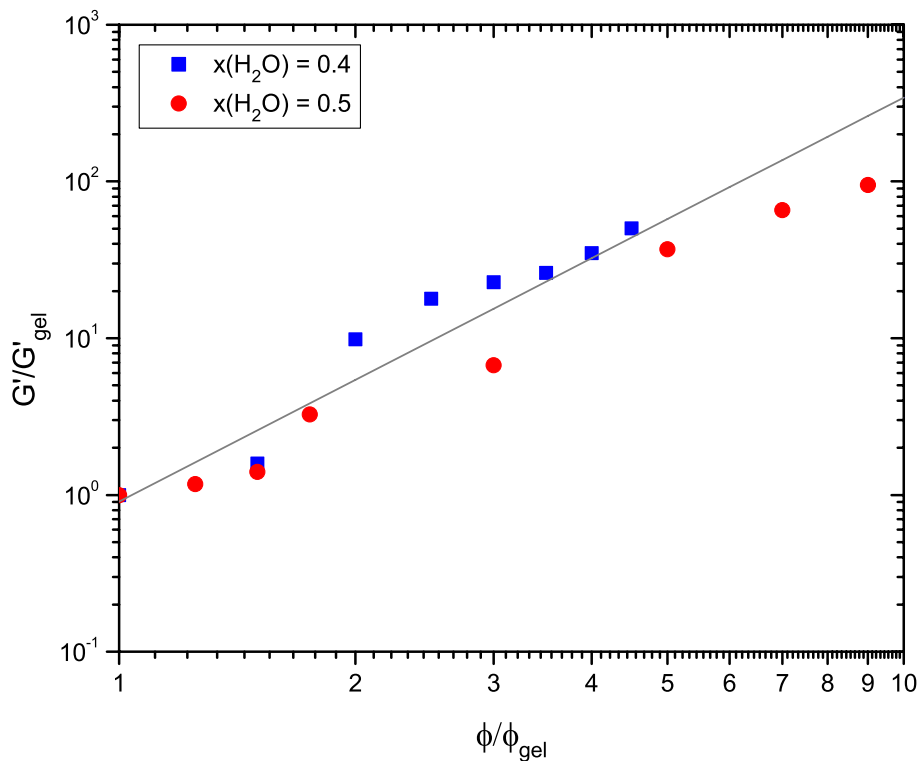


**Figure 6.** Generalized dependence of elastic modulus on Fmoc-FF volume fraction.  $G'_{gel}$  and  $\phi_{gel}$  represent the elastic modulus and Fmoc-FF concentration at the gel point, respectively. For  $x(H_2O) = 0.4$ :  $\phi_{gel} = 0.004$ ,  $G'_{gel} = 3318$  Pa; for  $x(H_2O) = 0.5$ :  $\phi_{gel} = 0.002$ ,  $G'_{gel} = 2710$  Pa.

As expected, a similar trend was observed for measured elastic moduli of gels of varying water concentrations at a fixed Fmoc-FF concentration – increasing water content led to stiffer gels and higher values of the elastic modulus. Experimental results for moduli of gels of different water content at two fixed Fmoc-FF concentrations (0.002 and 0.004) are given in Figure 7.

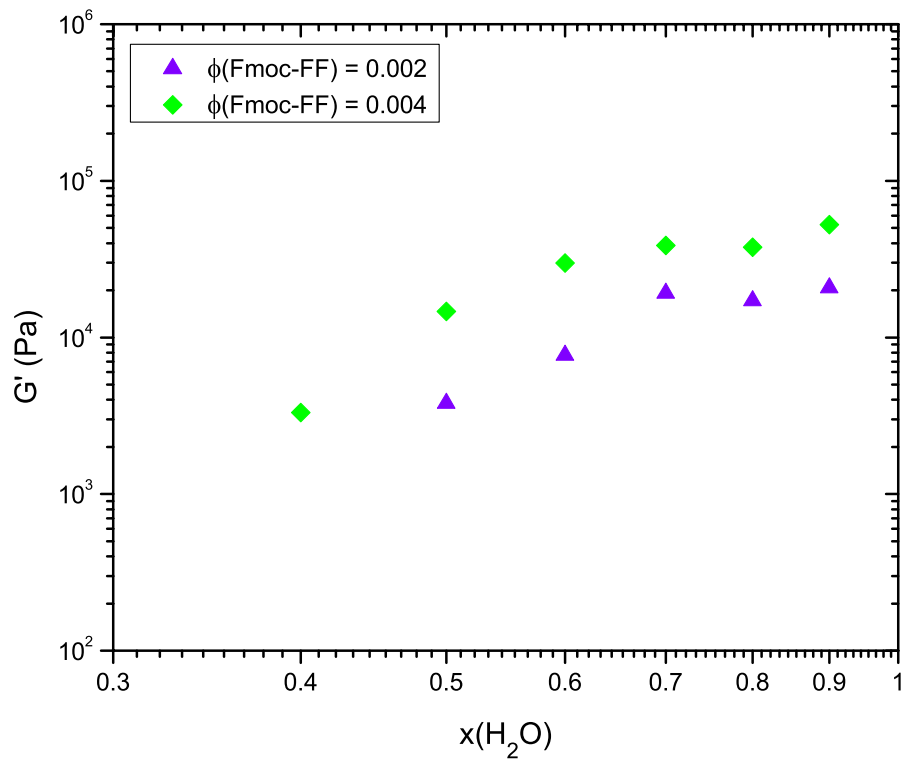


**Figure 7.** Dependence of elastic modulus on water concentration.

#### 4.2.3. Gel Reversibility

As described previously in section 3.5, gel reversibility was investigated by inducing high shear stress on the sample in order to cause it to yield. Figure 8 shows the results of a gel reversibility experiment on a sample of  $\phi(\text{Fmoc-FF}) = 0.01$  and  $x(\text{H}_2\text{O}) = 0.4$ .

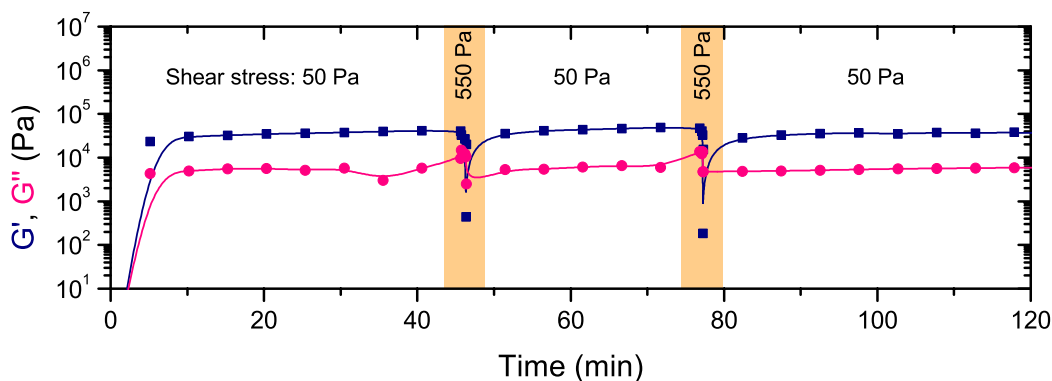


**Figure 8.** Reassembly of gel after mechanical disruption. When the shear stress is increased, the gel breaks and becomes a liquid ( $G' < G''$ ). When the shear stress is reduced, the gel rebuilds ( $G' > G''$ ) to its original mechanical strength.

The gel exhibited very good reversibility. It was found that after the gel has yielded into a liquid state, it successfully rebuilt to approximately the original value of its elastic modulus. This could be an indication that the system does not undergo spinodal decomposition, which would mean that Fmoc-FF gels are true equilibrium gels capable of full reversibility.

### 4.3. Comparison with Ultralocal Limit Model

As previously stated in section 2.2., localization theories were developed to describe equilibrium solution structures for spherical particles, allowing predictions of localization events, the volume fraction at the gel point  $\phi_{gel}$  as a function of strength of attraction (in this case, a function of water concentration) and particle size, as well as the prediction of the resulting elastic modulus at the gel point  $G'_{gel}$ . In the limit of low volume fractions, the mechanical properties of gels are expected to scale as  $G' \sim G'_{gel} \phi^x$ , where  $x$  is independent of volume fraction and strength of attraction.

### 4.3.1. Relating Strength of Attraction with Water Concentration and Gel Point Prediction

By applying the dynamic localization model in the ultralocal limit developed by Schweizer *et al.* (described in section 2.2.), the gel point volume fraction can be found. Below the gel point, the localization length is infinite, i.e.  $\sigma/r_L=0$ . At  $\phi_{gel}$ ,  $\sigma/r_L$  jumps to a finite value. For any fixed  $\phi_{gel}$ , we can vary  $\varepsilon/kT$  until the first finite value of  $\sigma/r_L$  is found as a solution of equation (2), corresponding to the localization length at the gel point ( $\sigma/r_L = \sigma/r_{L(gel)}$ ). Using this information, for a fixed  $\varepsilon/kT$ ,  $\phi$  is varied above the gel point  $\phi_{gel}$  and  $r_L$  is sought (Figure 9), which allows us to find the relationship between  $\varepsilon/kT$  and  $\phi_{gel}$  (Figure 10). By relating  $\varepsilon/kT$  vs.  $\phi_{gel}$  to the  $x(\text{H}_2\text{O})$  vs.  $\phi_{gel}$  experimental gel line (Figure 3), we determine how  $\varepsilon/kT$  varies with the water concentration, and the obtained relationship fits to a logarithmic dependence (Figure 11). Finally, the only remaining variable parameter is the particle size, which controls the magnitude of the elastic modulus. We find that the experimentally obtained magnitudes fit a model dependence calculated using a size of 8 nm (Figure 12).

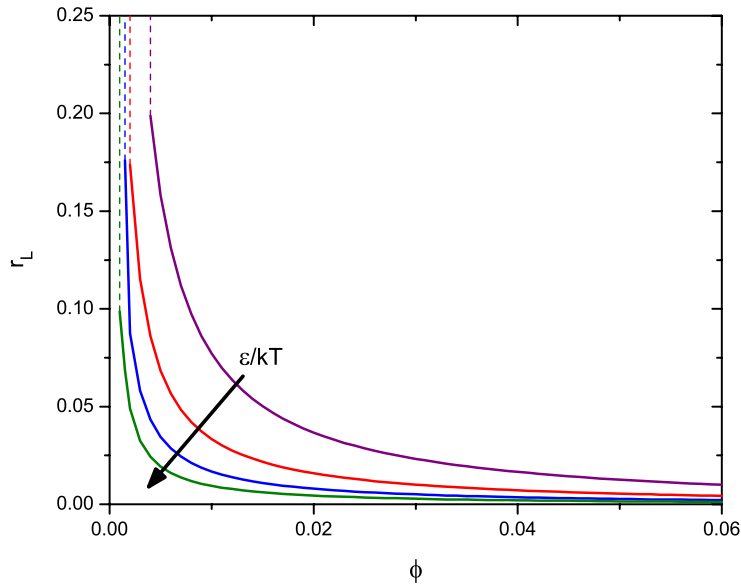


**Figure 9.** Dependence of localization length vs. volume fraction for increasing strength of attraction. The first finite value of  $r_L$  marks the gel point.

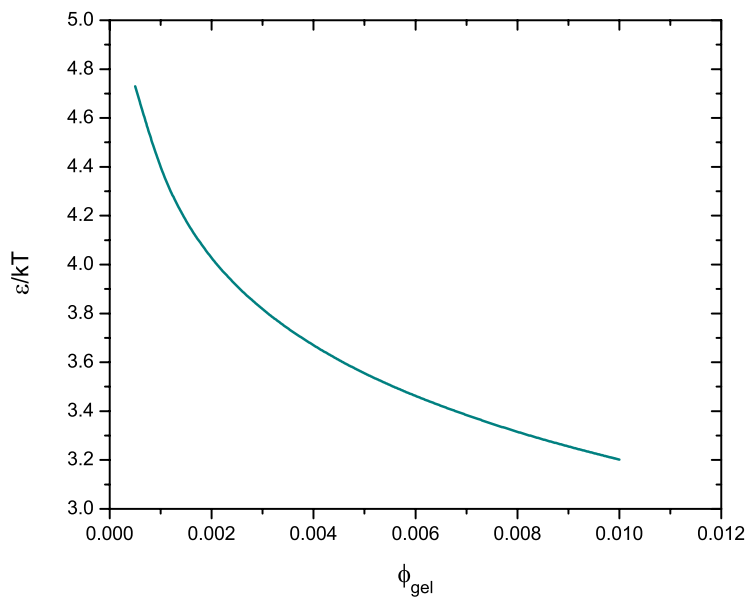


**Figure 10.** Change in strength of attraction with volume fraction at the gel point, predicted by the ultralocal limit model.

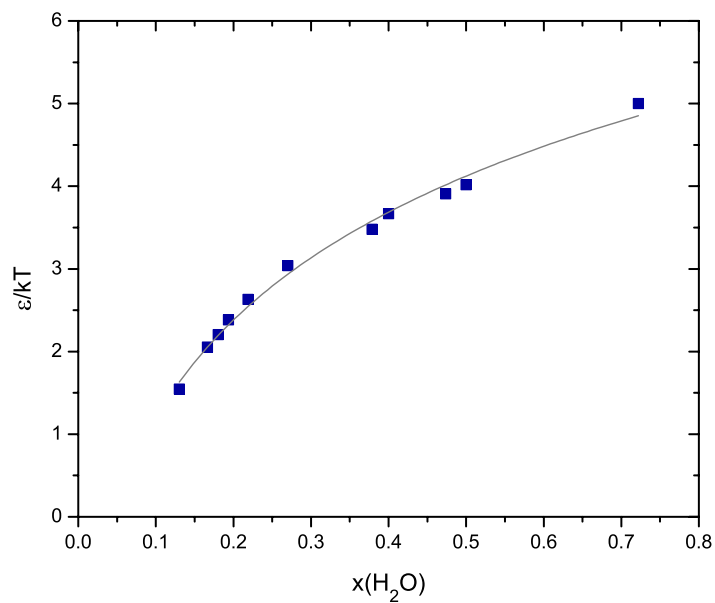


**Figure 11.** Strength of attraction as a function of gel water content, obtained based on the experimental solubility curve and theoretical predictions of the ultralocal MCT model.

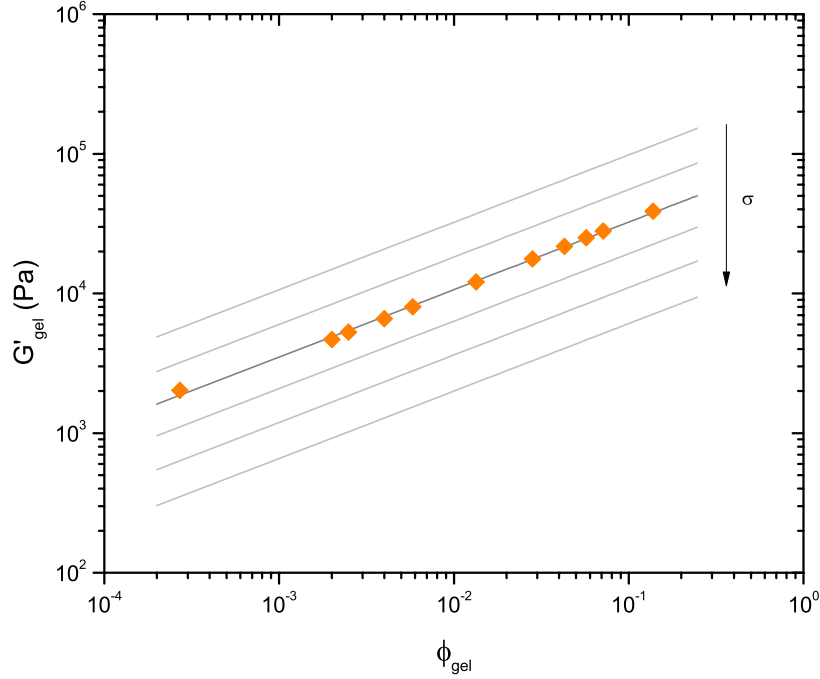


**Figure 12.** Predicted values of elastic modulus at gel points for varying particle size, obtained by the ultralocal MCT model. The model predicts  $G'_{gel}$  to have a power law dependence of  $\phi_{gel}$  with an exponent (slope) of  $\sim 0.5$ , which is also observed experimentally. The magnitudes of the predicted elastic modulus fit the experimental data for a particle size of 8 nm.

#### 4.3.2. Scaling Arguments and Elastic Modulus Prediction

The experimentally obtained values of elastic moduli for various Fmoc-FF concentrations and water contents were scaled by the values of elastic modulus at the gel point and the corresponding gel point volume fraction. When superimposed and plotted in a log-log diagram of  $G'/G'(\phi_{gel})$  vs.  $\phi/\phi_{gel}$ , the experimental data lie on approximately the same line of a power law fit, the slope of which is  $\sim 2.5$ . As mentioned previously in section 2.2, the ultralocal limit model by Schweizer *et al.* predicts an elastic modulus scaling of  $G' \sim \phi^3$ , while the Bergenholtz and Fuchs model predicts a scaling of  $G' \sim \phi^2$ .

This means that the elastic modulus behavior of the Fmoc-FF molecular gel lies somewhere in between the expectations of these two theoretical models.

This deviation may be explained by the fact that the mode coupling theory in the ultralocal limit gives a measure of elasticity per particle. However, the fibrous structure is expected to be composed of space spanning fibers, as well as dangling branches that do not contribute to the elasticity of the system. Therefore, an increase in volume fraction of Fmoc-FF molecules will not necessarily be followed by the predicted increase in rigidity resulting from the formation of a larger number of space filling fibers, because the addition of more particles is in part “spent” on the dangling bonds, which will not affect the elastic modulus. With this in mind, we can say that the elastic modulus scales as:

$$G' \sim \left( \begin{array}{c} \text{number of elastically active} \\ \text{bonds per unit volume} \end{array} \right) \times \left( \begin{array}{c} \text{elasticity} \\ \text{per bond} \end{array} \right)$$

We hypothesize that the number of elastically active bonds per unit volume scales as  $\sim \phi^{0.5}$ . If the elasticity per bond scales as  $\sim kT/r_L^2$ , taking into account equation (2), we have  $G' \sim \phi^{0.5}(\sigma/r_L)^2$ , resulting in  $G' \sim \phi^{2.5}$ . The  $\phi^{0.5}$  term allows for the possibility that the increase in Fmoc-FF volume fraction does not contribute only to the concentration of elastically active particles, but also the concentration of dangling bonds. A comparison between the experimental data and the ultralocal limit model prediction (Table 1) using the defined scaling yields a considerably good fit (Figure 13). As it can be seen, the model gives a reasonable estimate of the absolute magnitudes of the elastic modulus and a good prediction of the trend of the change in elastic behavior with the changes in Fmoc-FF and water concentrations.



**Table 1.** Predicted values of Fmoc-FF volume fraction and elastic modulus at the gel point for a range of water concentrations.

$x(\text{H}_2\text{O})$	$\phi_{\text{gel}}$	$G'_{\text{gel}}$ (Pa)
0.1	0.39015	62505.0
0.2	0.03457	19388.0
0.3	0.00837	9775.7
0.4	0.00306	6013.8
0.5	0.00140	4125.6
0.6	0.00074	3032.2
0.7	0.00043	2337.2
0.8	0.00027	1865.4
0.9	0.00018	1528.9

A second possible explanation can be that the anisotropic interactions and organization of the molecules results in a volume fraction dependence that is not captured in the ultralocal limit or the Yukawa low volume fraction approximation of Fuchs and Bergenholtz.

The essential predictions we can test are based on a separation of size and strength of attraction dependence from volume fraction dependence. The ability of simple models to capture the location of the gel and the magnitude of the modulus at the gel point suggests that the localization models hold promise for predicting the properties of molecular gels.

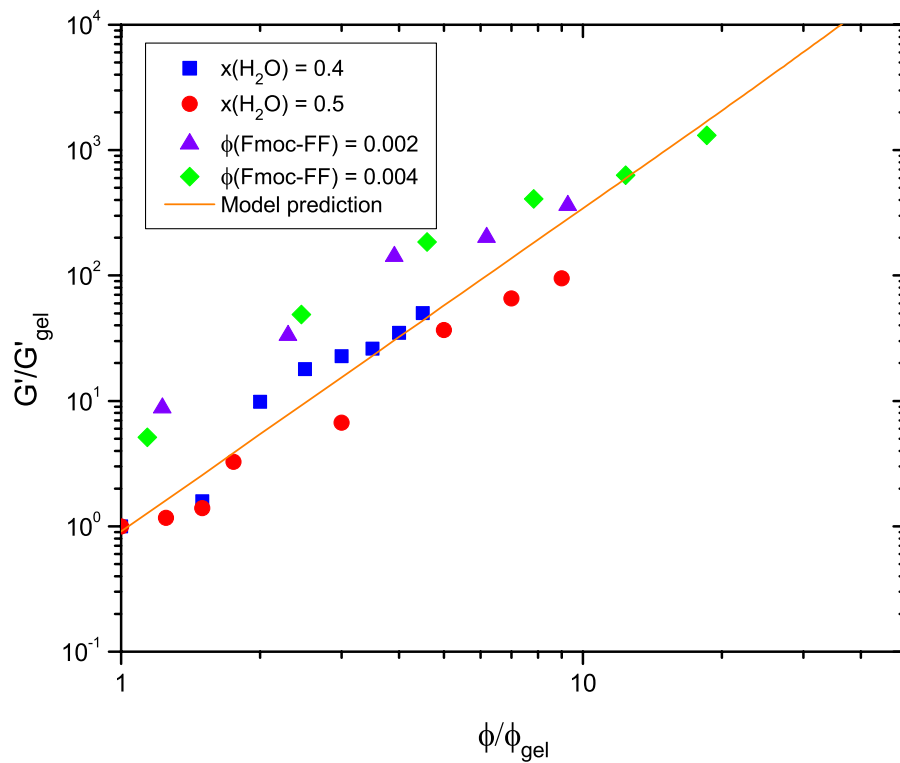


**Figure 13.** Comparison of experimentally determined elastic modulus data at two fixed Fmoc-FF volume fractions (0.002 and 0.004) and two fixed water concentrations (0.4 and 0.5) with the predictions of the ultralocal MCT model.

# CHAPTER 5. CONCLUSIONS

## 5.1. Experimental and Modeling Observations

The results presented here show that at room temperature molecules of Fmoc-diphenylalanine self assemble into rigid gels when dissolved in DMSO and mixed with water at very low concentrations. Upon mixing water with the DMSO Fmoc-diphenylalanine mixture, the solution goes opaque. Over time there is an opaque-to-clear transition during which time the solution gels. This process suggests that initial addition of water drives the Fmoc-diphenylalanine from solution and that over time there is a reorganization into a lower free energy state containing smaller objects that scatter less light but which grow to span space and product a gel. If the trigger here results in structures similar to the reported using a pH gelation trigger, the gel is formed of  $\pi$ -stacked molecules that assemble into branched fibrils A gelation curve was established by titration experiments. In order to decouple the influence of Fmoc-FF concentration and water concentration on the mechanical behavior of the resulting gels, rheological measurements were performed by keeping one of the concentrations fixed while varying the other, and vice versa. The results show that stiff gels can be formed at low volume fraction, exhibiting an increase in rigidity with increasing Fmoc-FF and water concentration. Furthermore, it was shown that the gels can rebuild to their original strength after yielding due to mechanical disruption, indicating characteristics of true equilibrium gels.

The dynamical localization model derived by Schweizer *et al.* based on mode coupling theory and the Yukawa model developed by Fuchs and Bergenholtz focus on different approximations for the effects of attraction on the point of localization. These models predict  $G' \sim G'_{gel}(\phi/\phi_{gel})^x$  with  $x = 2$  for the Yukawa interactions and  $x = 3$  for the ultralocal limit of spheres interacting with centrosymmetric pair potentials. Experimentally, these results demonstrate that  $G' \sim \phi^{2.5}$ . The fractional power law

observed experimentally may be attributed to the fibrous nature of the gel structure at low volume fraction and how the number density of elastically active particles grows with volume fraction. With this approach, a relationship between water concentration and strength of attraction was developed, predicting the gel point and the behavior of the elastic modulus of the gels. The model gave a reasonable fit of the experimental data when plotted as  $G'/G'(\phi_{gel})$  vs.  $\phi/\phi_{gel}$ , with data points of different Fmoc-FF and water concentrations all superimposing on the same power law curve.

## 5.2. Future Studies

One of the main questions that arise from the research conducted thus far is whether molecular gels based on dipeptide molecules such as Fmoc-FF can be considered as true equilibrium gels. While the reversibility of the gels upon yielding is certainly an indication of the possibility, further evidence of the absence of spinodal decomposition needs to be provided. One way to obtain this information is to perform small angle X-ray scattering (SAXS) and wide angle X-ray scattering (WAXS) measurements on the gel systems in order to observe the characteristic structures formed during the gelation process.

The phenomenon of the opaque-to-clear transition during the gel formation poses another interesting question about the structures that are formed when the dipeptide solution is initially mixed with water. An attempt will be made to observe the formation of the gel at different time frames using transmission electron microscopy (TEM). Additionally, this technique might provide some evidence to the hypothesis that the increase in Fmoc-FF volume fraction is partially spent on growth of dangling branch structures, and not only on space filling fibers.

Finally, more effort will be put into modeling of this type of systems. If it is possible to describe and predict the gel formation process and its behavior with changes in essential conditions, this knowledge could be used to synthesize similar molecules that

would allow the design of application-specific structural, optical, and biological functionality.

## REFERENCES

- [1] Zaccarelli, E. (2007). "Colloidal gels: equilibrium and non-equilibrium routes." *Journal of Physics: Condensed Matter* **19**(32): 323101.
- [2] Larson, R. G. (1999). *The structure and rheology of complex fluids*, Oxford University Press.
- [3] Henning-Winter, H. (2000). "The critical gel: the universal material state between liquid and solid", 99 NATO ASI Meeting, Les Houches, France.
- [4] Weiss, R. G. and Terech, P. (2006). "Molecular Gels: Materials with Self-Assembled Fibrillar Networks", Springer.
- [5] Jayawarna, V., et al. (2006). "Nanostructured Hydrogels for Three-Dimensional Cell Culture Through Self-Assembly of Fluorenylmethoxycarbonyl-Dipeptides." *Advanced Materials* **18**(5): 611-614.
- [6] Smith, A. M., et al. (2008). "Fmoc-Diphenylalanine Self Assembles to a Hydrogel via a Novel Architecture Based on  $\pi$ - $\pi$  Interlocked  $\beta$ -Sheets." *Advanced Materials* **20**(1): 37-41.
- [7] Tang, C., et al. (2009). "Fmoc-Diphenylalanine Self-Assembly Mechanism Induces Apparent pKa Shifts." *Langmuir* **25**(16): 9447-9453.
- [8] Ulijn, R. V. and A. M. Smith (2008). "Designing peptide based nanomaterials." *Chemical Society Reviews* **37**(4): 664-675.
- [9] Adams, D. J., et al. (2010). "Relationship between molecular structure, gelation behaviour and gel properties of Fmoc-dipeptides." *Soft Matter* **6**(9): 1971-1980.
- [10] Chen, L., et al. (2009). "Self-Assembly Mechanism for a Naphthalene- Dipeptide Leading to Hydrogelation." *Langmuir* **26**(7): 5232-5242.

- [11] Gazit, E. (2007). "Self-assembled peptide nanostructures: the design of molecular building blocks and their technological utilization." *Chemical Society Reviews* **36**(8): 1263-1269.
- [12] Haines-Butterick, L., et al. (2007). "Controlling hydrogelation kinetics by peptide design for three-dimensional encapsulation and injectable delivery of cells." *Proceedings of the National Academy of Sciences* **104**(19): 7791-7796.
- [13] Houton, K. A., et al. (2012). "On Crystal versus Fiber Formation in Dipeptide Hydrogelator Systems." *Langmuir* **28**(25): 9797-9806.
- [14] Liebmann, T., et al. (2007). "Self-assembling Fmoc dipeptide hydrogel for in situ 3D cell culturing." *BMC biotechnology* **7**(1): 88.
- [15] Mahler, A., et al. (2006). "Rigid, Self-Assembled Hydrogel Composed of a Modified Aromatic Dipeptide." *Advanced Materials* **18**(11): 1365-1370.
- [16] Rodriguez-Llansola, F., et al. (2012). "Structural and morphological studies of the dipeptide based l-Pro-l-Val organocatalytic gels and their rheological behaviour." *Soft Matter* **8**(34): 8865-8872.
- [17] Xie, Z., et al. (2009). "Shear-assisted hydrogels based on self-assembly of cyclic dipeptide derivatives." *Journal of Materials Chemistry* **19**(34): 6100-6102.
- [18] Reches, M. and E. Gazit (2003). "Casting metal nanowires within discrete self-assembled peptide nanotubes." *Science* **300**(5619): 625-627.
- [19] Kob, W., et al. (1997). *Experimental and Theoretical Approaches to Supercooled Liquids: Advances and Novel Applications (The Mode-Coupling Theory of the Glass Transition)*, ACS Books, Washington.
- [20] K. S. Schweizer and E. J. Saltzman (2003). *J. Chem. Phys.* 119, 1181.
- [21] E. J. Saltzman and K. S. Schweizer (2003). *J. Chem. Phys.* 119, 1197.
- [22] V. Kobelev and K. S. Schweizer (2005). *Phys. Rev. E* 71, 021401.

- [23] K. S. Schweizer (2005). J. Chem. Phys. 123, 244501.
- [24] E. J. Saltzman and K. S. Schweizer (2006). J. Chem. Phys. 125, 044509.
- [25] K. S. Schweizer and E. J. Saltzman (2004). J. Phys. Chem. B 108, 19729.
- [26] E. J. Saltzman and K. S. Schweizer (2006). Phys. Rev. E 74, 044509.
- [27] Y.-L. Chen and K. S. Schweizer (2004). J. Chem. Phys. 120, 7212.
- [28] Y.-L. Chen, V. Kobelev, and K. S. Schweizer (2005). Phys. Rev. E 71, 041405.
- [29] V. Kobelev and K. S. Schweizer (2005). J. Chem. Phys. 123, 164902.
- [30] G. Yatsenko and K. S. Schweizer (2007). J. Chem. Phys. 126, 014505.
- [31] Schweizer, K. S. and G. Yatsenko (2007). "Collisions, caging, thermodynamics, and jamming in the barrier hopping theory of glassy hard sphere fluids." The Journal of Chemical Physics **127**(16): 164505-164509.
- [32] Bergenholtz, J. and M. Fuchs (1999). "Gel transitions in colloidal suspensions." Journal of Physics: Condensed Matter **11**(50): 10171.